Photothermal rate-window spectrometry for noncontact bulk lifetime measurements in semiconductors

Z. H. Chen, R. Bleiss,[a] and A. Mandelis
Photothermal and Optoelectronic Diagnostics Laboratory, Department of Mechanical Engineering, and Ontario Laser and Lightwave Research Center, University of Toronto, 5 King's College Road, Toronto, Ontario M5S 1A4 Canada

A. Buczkowski and F. Shimura
Department of Materials Science and Engineering, North Carolina State University, Raleigh, North Carolina 27695-7916

(Received 29 September 1992; accepted for publication 21 January 1993)

A new noncontact technique for the determination of excess carrier lifetimes in semiconductors is presented. The technique employs a square laser pulse ($h\nu > E_g$) and measures the infrared photothermal radiometric response of the sample. By applying the photothermal rate-window concept, the excess photoexcited carrier bulk lifetime was measured with optimal signal-to-noise (S/N) ratio and simple, unambiguous interpretation from the maximum position of the rate-window signal. The technique has been applied to Au-, Fe-, and Cr-doped Czochralski silicon crystals. The experimental results from boxcar and lock-in rate-window methods were found to agree very well. The results are further mostly in agreement with those from the noncontact laser/microwave detection method.

I. INTRODUCTION

The measurement of photoexcited excess carrier lifetime is useful in characterizing the quality of semiconductor materials and modeling semiconductor devices. Besides the conventional photoconductive technique for carrier lifetime measurement, many recently developed noncontact, nondestructive techniques have drawn particular interest.[1,2] Photothermal radiometry (PTR),[3] laser/microwave absorption/reflection (LMR),[4–6] infrared absorption (IA),[7–9] photoconductance (PC),[10] or open-circuit voltage decay (OCVD)[11] are among those techniques commonly used for noncontact carrier lifetime studies. In all these methods laser illumination is used to generate excess electron-hole pairs. The resulting signal is detected in the frequency-domain as a function of modulation frequency (in PTR) or in the time-domain as a transient signal (IA, LMR, PC, and OCVD).

In this article, a new noncontact photothermal rate-window method is presented. The technique utilizes a time-gated Ar^+-ion laser beam ($\lambda = 514$ nm) to generate excess carriers at or near the surface, and measures the resulting photothermal radiometric transient signal using an IR detector. The experimental results on excess carrier bulk lifetimes of Fe-, Cr-, and Au-doped CZ silicon wafers show good agreement with the theoretical analysis and partial agreement with the results measured with the laser/microwave detection method.[8]

II. THEORETICAL ANALYSIS OF THE PHOTOTHERMAL RATE-WINDOW SPECTROMETRIC SIGNAL

Photothermal rate-window spectrometry was introduced as a technique suitable for measuring thermophysical material properties from photothermal radiometric transient signals.[12,13] Photothermal radiometry is a well-established method for the study of thermal properties of solid materials in a nondestructive and noncontact fashion,[14–17] and it has also been widely used with great success in the analysis of semiconductor materials.[3,18] In this section, we discuss the theoretical principles of the semiconductor excess carrier lifetime measurement using infrared photothermal radiometry.

The configuration of our mathematical model is shown in Fig. 1. The semiconductor sample is assumed semi-infinite (the validity of the assumption will be discussed in a later section), and the sample is irradiated with a repetitive square laser pulse of duration τ_p and period T_0. The photon energy $h\nu$ of the laser beam is greater than the semiconductor energy gap, E_g, and the excess minority-carrier density is small compared to the majority-carrier density (low-injection limit). The photoexcited excess carrier density, $\Delta N(z,t)$, is given by solving the carrier continuity equation[19]

$$D\frac{\partial^2 \Delta N(z,t)}{\partial z^2} - \frac{\Delta N(z,t)}{\tau} + G(z,t) = \frac{\partial \Delta N(z,t)}{\partial t}. \qquad (1)$$

Here D (m^2/s) is the ambipolar diffusion coefficient, τ (s) the carrier bulk lifetime, and $G(z,t)$ ($1/m^3$ s) the carrier generation rate, which is given by

$$G(z,t) = \begin{cases} \dfrac{\alpha \eta I_0 e^{-\alpha z}}{h\nu}; & t < \tau_p \\ 0; & t > \tau_p. \end{cases} \qquad (2)$$

The square laser pulse (intensity I_0: W/m^2) illuminates the sample surface and is absorbed throughout the sample with an absorption coefficient α ($1/m^{-1}$) and quantum efficiency η.

The appropriate initial and boundary conditions are

[a]On leave from Jenoptik GmbH, Jena, Germany.

Downloaded 18 Jul 2008 to 128.100.49.17. Redistribution subject to AIP license or copyright; see http://jap.aip.org/jap/copyright.jsp

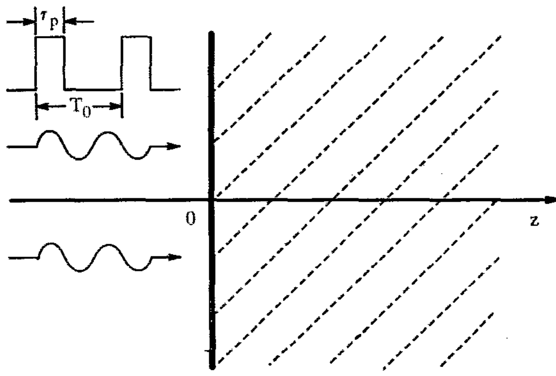

FIG. 1. Schematic configuration of the PTR rate-window signal model involving a square laser pulse of duration τ_p and period T_0, and a semi-infinite photoexcited semiconductor.

$$\Delta N(z,0)=0 \tag{3}$$

and

$$D\frac{\partial\Delta N(z,t)}{\partial z}\bigg|_{z=0}=s_1\Delta N(z,t). \tag{4}$$

Here s_1 (m/s) is the carrier surface recombination velocity at the front surface of the semiconductor. The former (initial) condition indicates that there is no significant free carrier concentration before the onset of the optical pulse.

Equation (1) can be solved in the Laplace domain and the resulting expression for the excess carrier density is

$$\Delta N(z,s)=\frac{\alpha\eta I_0}{h\nu D}\frac{1-e^{-s\tau_p}}{s[\alpha^2-\sigma_e^2(s)]}\left(\frac{D\alpha+s_1}{D\sigma_e(s)+s_1}e^{-\sigma_e(s)z}-e^{-\alpha z}\right) \tag{5}$$

with

$$\sigma_e(s)=\frac{1}{\sqrt{D}}(s+\tau^{-1})^{1/2}. \tag{6}$$

The boundary condition, Eq. (4), indicates the absence of free-carrier contributions to Eq. (5) due to diffusive plasma reflections from the back surface of an actual sample, at distance ℓ from $z=0$. Consideration of semiconductor samples of finite thickness, ℓ, with the addition of a back-surface boundary condition similar to Eq. (4), contributes a multiplicative term to the Laplace domain Eq. (5) of the form[20]

$$\frac{1}{1-e^{-2\sigma_e(s)l}}, \tag{7}$$

the result of infinite inter-reflections. The most important effect of this modification to the theory presented here is a contribution to the average free carrier density, proportional to

$$1+e^{-2\sigma_e(s)l}. \tag{8}$$

The exponential in this expression can be neglected with respect to unity for observation times t such that $2\sigma_e(s)\ell \gg 1$. From Eq. (6) and the correspondance $s \Leftrightarrow 1/t$, we conclude that for $t>\tau$, which is the case in our experiments, the necessary condition for neglecting the ℓ-dependent diffusional reflections is

$$\tau \ll \frac{4l^2}{D}. \tag{9}$$

This condition was satisfied for all our experiments with $\tau \leqslant 20\ \mu$s and $4\ell^2/D > 330\ \mu$s, corresponding to silicon wafers of 500 μm thickness and carrier diffusivity $D=30$ cm^2/s.[21]

In photothermal radiometry the infrared emission signal, S_{IR} from the semiconductor can be calculated by applying Kirchhoff's radiation law under nonequilibrium carrier conditions.[22] As every excess carrier acts as an independent black body radiator, the signal level S_{IR} is proportional to the spatially integrated carrier density. Integrating Eq. (5) over the semiconductor sample thickness and transforming it back from the Laplace domain to the time domain, one can get

$$S_{IR}=\begin{cases}F_{IR}(t;\tau,\tau_\alpha,\tau_s); & t\leqslant\tau_p\\ F_{IR}(t;\tau,\tau_\alpha,\tau_s)-F_{IR}(t-\tau_p;\tau,\tau_\alpha,\tau_s); & t\geqslant\tau_p,\end{cases} \tag{10}$$

where

$$F_{IR}(t;\tau,\tau_\alpha,\tau_s)=C\zeta\frac{\eta I_0}{h\nu}\frac{1}{\sqrt{\tau_s}-\sqrt{\tau_\alpha}}\left\{\frac{\sqrt{\tau_s}}{\tau_s^{-1}-\tau^{-1}}\left[\sqrt{\frac{\tau}{\tau_s}}\,\mathrm{erf}\left(\sqrt{\frac{t}{\tau}}\right)+e^{-t/\tau}W\left(\sqrt{\frac{t}{\tau_s}}\right)-1\right]-\frac{\sqrt{\tau_\alpha}}{\tau_\alpha^{-1}-\tau^{-1}}\times\left[\sqrt{\frac{\tau}{\tau_\alpha}}\,\mathrm{erf}\left(\sqrt{\frac{t}{\tau}}\right)+e^{-t/\tau}W\left(\sqrt{\frac{t}{\tau_\alpha}}\right)-1\right]\right\}. \tag{11}$$

Here ζ is a constant related to the infrared radiation detector,[18] and C is a constant independent of any photoexcited carrier characteristic time constants, i.e., Eqs. (12)–(13) below.

$$\tau_\alpha=\frac{1}{\alpha^2 D} \tag{12}$$

is the time required for a carrier to diffuse to a depth equal to the optical absorption length, $1/\alpha$. Similarly,

$$\tau_s=\frac{D}{s_1^2} \tag{13}$$

is a time constant due to recombination at surface defects, which is dependent on surface recombination velocity and carrier diffusion coefficient.

$$W(z)=e^{z^2}\,\mathrm{erfc}(z) \tag{14}$$

is a function encountered in time-domain diffusion-type problems,[12,23] where erfc(z) is the complementary error function defined by

$$\mathrm{erfc}(z)=\frac{2}{\sqrt{\pi}}\int_z^\infty e^{-q^2}dq. \tag{15}$$

For opaque semiconductors in which $\tau_\alpha \ll \tau$, and $\tau_\alpha \ll \tau_s$, Eq. (8) can be simplified to

Downloaded 18 Jul 2008 to 128.100.49.17. Redistribution subject to AIP license or copyright; see http://jap.aip.org/jap/copyright.jsp

$$F_{IR}(t;\tau,\tau_s)=C\zeta\frac{\eta I_0}{h\nu}\frac{1}{\tau_s^{-1}-\tau^{-1}}\left[\sqrt{\frac{\tau}{\tau_s}}\,\mathrm{erf}\left(\sqrt{\frac{t}{\tau}}\right)+e^{-t/\tau}W\left(\sqrt{\frac{t}{\tau_s}}\right)-1\right]. \tag{16}$$

In the special case of very low surface recombination velocity ($s_1\rightarrow 0$, i.e., $\tau_s\gg\tau$), Eq. (16) can be further simplified.

It is evident from Eq. (17) that the infrared radiometric signal is a pure exponential function dependent on the bulk lifetime τ only, when the carrier surface recombination

$$F_{IR}(t;\tau)=C\zeta\frac{\eta I_0}{h\nu}\tau(1-e^{-t/\tau}) \tag{17}$$

velocity is very low. In what follows, we will concentrate on the discussion of this case, which implies high quality material surfaces, such as those present in our experiments. In the case where s_1 is not negligible, our simulations of the full Eq. (11) and other theoretical and experimental results[21,24] show that a single exponential cannot describe the early time-decay of the free photoexcited carrier density. That decay profile is faster than the exponential. Therefore, in our analysis purely exponential decay has been used as the unambiguous criterion for the photothermal (PTR) signal domination by a bulk type of carrier recombination mechanism alone.

III. BOXCAR AND LOCK-IN RATE-WINDOW PHOTOTHERMAL SPECTROMETRY

As discussed in the previous section, when the carrier surface recombination velocity is very low, the PTR signal in the opaque regime is a pure exponential function

$$S_{IR}(t;\tau)=C\zeta\frac{\eta I_0}{h\nu}\tau\begin{cases}1-e^{-t/\tau}; & t\leqslant\tau_p\\ (e^{\tau_p/\tau}-1)e^{-t/\tau}; & t\geqslant\tau_p.\end{cases} \tag{18}$$

In this case, the carrier bulk recombination lifetime can be measured by using boxcar and/or lock-in rate-window spectrometry.

In the boxcar rate-window method, the rate-window is applied only to the decay portion of the transient. Therefore the pulse duration, τ_p, does not affect the maximum of the resulting rate-window signal. Upon taking $\partial[S_{IR}(t_1;\tau)-S_{IR}(t_2;\tau)]/\partial\tau=0$, we obtain

$$\tau=\frac{t_2-t_1}{\ln(t_2/t_1)}, \tag{19}$$

where the decaying transient is measured at two times t_1 and t_2.

The lock-in rate-window method has the advantage of combining the superior signal-to-noise ratio of a tuned electronic filter, familiar with frequency-domain PTR detection, with the simple and straightforward interpretation of the time-domain PTR signal in terms of electron-hole recombination time delays. In the lock-in rate-window method, we measure the in-phase (IP) signal resulting from the lock-in amplifier, which amounts to the fundamental Fourier component b_1 of $S_{IR}(t;\tau)$[12] over the pulse repetition period T_0:

$$\begin{aligned}b_1(\tau;T_0)&=\frac{2}{T_0}\int_0^{T_0}S_{IR}(t;\tau)\sin(\omega_0 t)dt\\&=C\zeta\frac{2\eta I_0}{\pi^2 h\nu}\tau\bigg(1-\cos(\omega_0\tau_p)\\&\quad+\frac{\omega_0}{\sqrt{\tau^{-2}+\omega_0^2}}[\sin(\omega_0\tau_p+\theta)\\&\quad-(1+e^{-(T_0-\tau_p)/\tau}-e^{-T_0/\tau})\sin\theta]\bigg),\end{aligned} \tag{20}$$

where

$$\theta=\tan^{-1}(\omega_0\tau);\quad \omega_0=\frac{2\pi}{T_0}. \tag{21}$$

Equation (20) has a maximum if the measurement is performed at a constant temperature (therefore τ is a constant in this case) and the repetition period T_0 of the laser pulse is varied. Now, the IP component of the lock-in output is obtained by weighting the fundamental Fourier coefficient $b_1\sin(\omega_0 t)$ by the square-wave lock-in reference function of duration $T_0,e_r(t)$, phase-tuned so as to align the origin of all times at $t=0$. This corresponds to setting the positive (or negative) edge of the reference square-wave in-phase with the rising edge of the optical pulse.[13] The result of this operation under long lock-in filter time constant is

$$\begin{aligned}S_{IP}(\tau,T_0)&=\frac{1}{T_0}b_1(\tau,T_0)\int_0^{T_0}\sin(\omega_0 t)e_r(t)dt\\&=\frac{2}{\pi}b_1(\tau,T_0).\end{aligned} \tag{22}$$

In this case, from the condition for the existence of an extremum:

$$\frac{\partial b_1(\tau;T_0)}{\partial T_0}=0 \tag{23}$$

one obtains numerically

$$(T_0)_{max}=2.5681\tau+1.9973\tau_p, \tag{24}$$

i.e., when scanning the repetition period of the laser pulse ($T_0>\tau_p$), the period $(T_0)_{max}$ at which a rate-window signal maximum occurs is very simply determined by the carrier bulk lifetime τ and the pulse duration τ_p only, provided that the surface recombination lifetime τ_s is long (and thus not recombination rate-limiting). The simplicity of Eq. (24), in conjunction with the superior S/N ratio afforded by the narrow-band lock-in detection,[13] demonstrates the distinct advantages of the photothermal lock-in rate-window technique over the boxcar method described earlier.

Downloaded 18 Jul 2008 to 128.100.49.17. Redistribution subject to AIP license or copyright; see http://jap.aip.org/jap/copyright.jsp

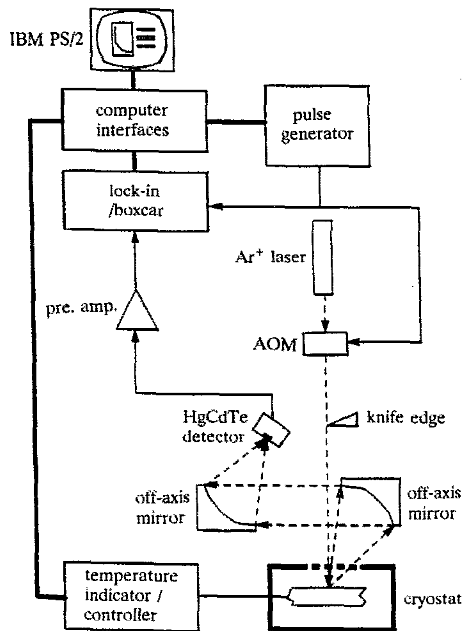

FIG. 2. Experimental system of photothermal rate-window spectrometry.

IV. EXPERIMENTAL RESULTS

The experimental setup for rate-window photothermal radiometry is shown in Fig. 2. A pulsed laser beam obtained by modulating a cw Ar^+-ion laser using an acousto-optic modulator was slightly focused on the sample to the size of approximately 1 mm diameter. The resulting infrared radiation emitted from the sample surface was collected by two off-axis paraboloidal mirrors and detected using a liquid N_2-cooled photoconductive mercury-cadmium-telluride (MCT) detector. The frequency bandwidth of the MCT detector-preamplifier system was 5 Hz–1.5 MHz, capable of capturing PTR decay events on the order of ~ 0.7 μs and longer, i.e., well within the observed 0.9–22.9 μs recombination lifetime range. Faster decays may also be monitored using photovoltaic MCT detectors. According to the method for setting up a rate-window, the transient was then directed to a lock-in amplifier for photothermal lock-in rate-window spectrometry, or to a boxcar averager (or a digitizer to save the transients in the computer memory and using the computer to play the role of the boxcar averager) for photothermal boxcar rate-window spectrometry. The setup also has a capacity to measure the temperature dependence of bulk lifetimes by using a cryostat. A set of *n*- and *p*-type Si samples intentionally contaminated with deep-level forming Cr, Fe, and Au metals during Czochralski crystal growth, was studied using the technique. The wafers were RTA cleaned and oxidized to minimize the effect of surface recombination. The properties of the silicon wafers studied are summarized in Table I.

The optical absorption coefficient of intrinsic Si is given by Dash and Newman.[25] For the Ar^+-ion laser ($\lambda = 514$ nm; 2.41 eV) radiation used in our system, the absorption coefficient is $\sim 10^4$ cm^{-1}, or the optical

TABLE I. Properties of silicon wafers used in this study (CZ⟨100⟩ 65 mm diameter).

Sample	Metal impurity	Resistivity (Ω cm)	Oxygen conc. (ppma)	Conc. of metal (atoms/cm^3)$\times 10^{12}$
N4	Cr	5–13	11.8	17
N5	Fe	6–16	14.5	47
N11	Au	4–13	17.2	11
P4	Cr	11–15	11.6	16
P5	Fe	9–13	15.4	61
P11	Au	10–15	14.2	31

absorption length is ~ 1 μm which is much less than the sample thickness of ~ 500 μm. Therefore we can consider that the sample is optically semi-infinite and totally opaque ($\tau_\alpha = 3.33 \times 10^{-10}$ s, much less than the earliest experimental time considered in this work).

Figure 3 is a transient signal from a Cr-doped *n*-type Si sample (N4). The linearity of the semi-logarithmic plot in Fig. 3 indicates that the carrier surface recombination velocity of the sample is very low as the signal conforms to the simple case described by Eqs. (17) and (18).

A boxcar rate-window signal of the same Cr-doped *n*-type Si sample (N4) is shown in Fig. 4. In that figure, the two gate times of the boxcar were chosen as $t_2/t_1 = 2$ and the horizontal axis is the gate time t_1. From the $(t_1)_{max}$ ($=15$ μs) where the maximum rate-window signal occurs, one can obtain the carrier bulk lifetime $\tau = 21.6$ μs according to Eq. (19). Table II summarizes the experimental results using this method.

Figure 5 shows the lock-in rate-window in-phase signals of the Fe-doped *n*-type Si sample (N5) with several pulse durations ($\tau_p = 10$, 50, 100, and 200 μs). The curves are normalized at the peak of curve (d) ($\tau_p = 200$ μs). The $(T_0)_{max}$ where the maximum rate-window signals occur are 45, 130, 227, and 430 μs, respectively. From Eq. (24) one obtains the carrier bulk lifetime $\tau = 9.7$, 11.7, 10.6, and 11.9 μs. The solid lines are the theoretical simulation using Eq. (20) with carrier bulk lifetime $\tau = 11$ μs. No other adjustments were introduced in the theoretical simulations to all four experimental data curves. Even better fits could

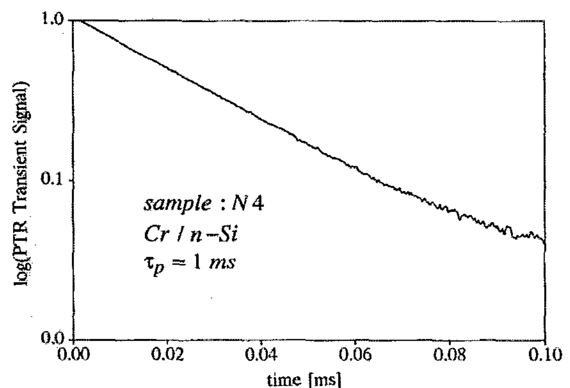

FIG. 3. Photothermal transient of the Cr-doped Si sample (N4) in logarithmic scale.

Downloaded 18 Jul 2008 to 128.100.49.17. Redistribution subject to AIP license or copyright; see http://jap.aip.org/jap/copyright.jsp

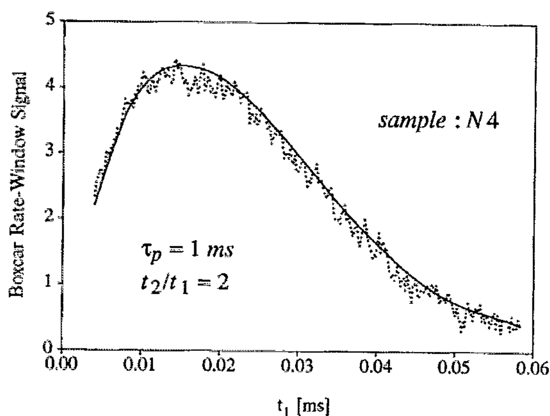

FIG. 4. Boxcar rate-window signal of Cr-doped *n*-type Si sample (N4). Total number of averaged transients: 2500. The dotted line is the experimental result and the solid line is the smoothed curve of the experimental data.

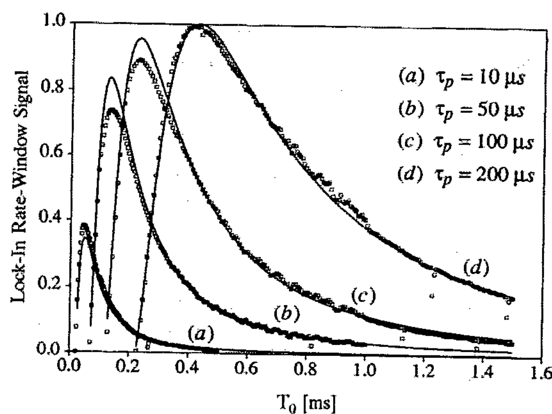

FIG. 5. Lock-in rate-window signals of the Fe-doped *n*-type Si sample (N5) with four different pulse durations. The solid lines are theoretical simulations using Eq. (20) with $\tau=11$ μs. Lock-in filter time constant: 1 s.

have been obtained with individual curve adjustments. The lock-in rate-window in-phase signals of Cr-, Fe-, Au-doped *p*-Si wafers are shown in Fig. 6. This figure shows the excellent resolution of the lock-in rate-window detection technique, concerning the determination of the values of the photoexcited carrier bulk recombination lifetime from the curve maxima. The superior S/N ratio lock-in rate-window[13] determination of the maximum in the fundamental Fourier component of the photothermal transient has a τ resolution of 1 μs, limited only by the dynamic range of the data acquisition system. An order of magnitude improvement is expected with an extended dynamic range system timing controller. The measured carrier bulk lifetimes are summarized in Table III, which also includes values of τ obtained by the laser/microwave reflection technique.[8,9] These results are consistent with each other with some notable exceptions. The consistent results further agree fairly well with the results measured with the boxcar rate-window method. The results on wafers N5, N11, and P4 also agree with those obtained from the laser/microwave detection method. With regard to a few discrepancies in Table III, we found that for Au-doped Si wafers (both *n*-type, N11, and *p*-type, P11, materials) the bulk lifetime measured by using a laser beam with pulse duration $\tau_p=50$ μs is much smaller than other measured values by using shorter pulse durations. Upon further investigation of the transient signals from Au-doped samples with various pulse durations, it was found that the transient decay becomes nonexponential when the pulse duration is at least one order of magnitude longer than the bulk lifetime of Au-doped wafers. The origin of this phenomenon is unclear and is under further study.

TABLE II. Experimental results of carrier bulk lifetimes measured using the PTR boxcar rate-window method.

Sample	N4	N5	N11	P4	P5	P11
τ (μs)	21.6	11.7	5.1	21.6	5.5	2.7

V. SUMMARY

A new noncontact photothermal rate-window spectrometry for measuring excess carrier bulk lifetime in electronic materials is presented in this article. Experimentally, the excess electron-hole pairs are generated by a laser pulse, and the transient photothermal radiation decay curves are measured by using an IR detector and analyzed with boxcar time-gated detection or a lock-in amplifier. The carrier bulk lifetime is then easily and sensitively measured from the peak of the rate-window signal.

The lock-in rate-window method has a significant advantage over the boxcar method in terms of signal-to-noise ratio. Experimentally the lock-in rate-window method has a more clearly defined maximum signal (i.e., higher resolution) and needs less time to perform the experiment than the boxcar method, which requires more signal averaging time to obtain an acceptable S/N ratio with our present instrumentation. Therefore, the lock-in rate-window method coupled to PTR is ideally suitable for noncontact electronic measurements with low signal levels, especially at low temperatures where the photothermal radiometric

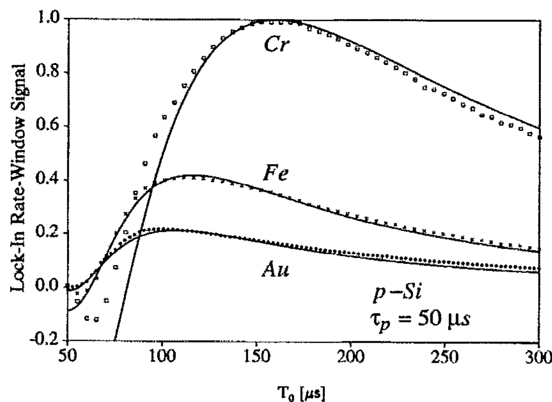

FIG. 6. Lock-in rate-window signals of Cr-, Fe-, and Au-doped *p*-Si wafers with pulse duration $\tau_p=50$ μs. The solid lines are theoretical simulations.

Downloaded 18 Jul 2008 to 128.100.49.17. Redistribution subject to AIP license or copyright; see http://jap.aip.org/jap/copyright.jsp

TABLE III. Experimental results of carrier bulk lifetimes (in μs) measured using the PTR lock-in rate-window method.

τ_p (μs)	N4	N5	N11	P4	P5	P11
10	8.2	9.7	5.3	22.9	7.0	3.1
30	14.4	12.9	4.0	21.1	6.1	2.4
50	16.8	11.7	1.5	22.2	6.3	0.9
	23.0[a]	12.2[a]	4.8[a]	0.6[b]	0.6[b]	1.1[b]
	18.0[c]	11.0[c]	4.5[c]	8.2[c]	0.6[c]	1.1[c]

[a]Results measured with laser/microwave technique (see Ref. 8) at 250 K.
[b]Results measured with laser/microwave technique (see Ref. 9) at 300 K.
[c]Recent measurements with laser/microwave technique (this work).

signal is small due to the Stefan–Boltzmann radiation law (T^4 dependence). The technique may further be implemented with thin electronically active layers, provided that a full model with finite boundaries replaces Eq. (11). This generalization is currently under investigation.[20]

ACKNOWLEDGMENTS

The support of the Ontario Laser and Lightwave Research Center (OLLRC), the Natural Sciences and Engineering Research Council of Canada (NSERC), and of Jenoptik GmbH, Jena, Germany, is gratefully acknowledged.

[1] D. K. Schroder, *Semiconductor Material and Device Characterization* (Wiley, New York, 1990).
[2] J. W. Orton and P. Blood, *The Electrical Characterization of Semiconductors: Measurement of Minority Carrier Properties* (Academic, San Diego, 1990).
[3] S. J. Sheard, M. G. Somekh, and T. Hiller, Mater. Sci. Eng. B **5**, 101 (1990).
[4] T. Warabisako, T. Saitoh, T. Motooka, and T. Tokuyama, Jpn. J. Appl. Phys. Suppl. **22-1**, 557 (1982).
[5] J. Waldmeyer, J. Appl. Phys. **63**, 1977 (1988).
[6] Z. G. Ling and P. K. Ajmera, J. Appl. Phys. **69**, 519 (1991).
[7] Y. Mada, Jpn. J. Appl. Phys. **18**, 2171 (1979).
[8] F. Shimura, T. Okui, and T. Kusama, J. Appl. Phys. **67**, 7168 (1990).
[9] A. Buczkowski, G. A. Rozgonyi, and F. Shimura, Proc. MRS Spring Conf. (1992).
[10] T. Tiegje, J. I. Haberman, R. W. Francis, and A. K. Ghosh, J. Appl. Phys. **54**, 2499 (1983).
[11] U. Lehmann and H. Foll, J. Electrochem. Soc. **135**, 2831 (1988).
[12] A. Mandelis and Z. H. Chen, Rev. Sci. Instrum. **63**, 2977 (1992).
[13] Z. H. Chen and A. Mandelis, Phys. Rev. B **46**, 13526 (1992).
[14] P. E. Nordal and S. O. Kanstad, Physica Scripta **20**, 659 (1979).
[15] R. Santos and L. C. M. Miranda, J. Appl. Phys. **52**, 4192 (1981).
[16] R. D. Tom, E. P. O'Hara, and D. Benin, J. Appl. Phys. **53**, 5392 (1982).
[17] W. P. Leung and A. C. Tam, J. Appl. Phys. **56**, 153 (1984).
[18] I. Little, G. M. Crean, and S. J. Sheard, Mater. Sci. Eng. B **5**, 89 (1990).
[19] J. P. McKelvey, *Solid State and Semiconductor Physics* (Krieger, Malabar, FL, 1966), Chap. 10.
[20] A. Mandelis (unpublished).
[21] K. L. Luke and L-J. Cheng, J. Appl. Phys. **61**, 2282 (1987).
[22] J. C. White and J. G. Smith, J. Phys. E **10**, 817 (1977).
[23] A. Mandelis and B. S. H. Royce, J. Appl. Phys. **50**, 4330 (1979).
[24] A. Buczkowski, Z. J. Radzimski, G. A. Rozgonyi, and F. Shimura, J. Appl. Phys. **69**, 1 (1991).
[25] W. C. Dash and R. Newman, Phys Rev. **99**, 1151 (1955).

Downloaded 18 Jul 2008 to 128.100.49.17. Redistribution subject to AIP license or copyright; see http://jap.aip.org/jap/copyright.jsp